Focusing of nitric oxide mediated nitrosation and oxidative nitrosylation as a consequence of reaction with superoxide

Michael G. Espey*, Douglas D. Thomas, Katrina M. Miranda, and David A. Wink

Radiation Biology Branch, National Cancer Institute, National Institutes of Health, Bethesda, MD 20892

Edited by Louis J. Ignarro, University of California, Los Angeles School of Medicine, Los Angeles, CA, and approved May 29, 2002 (received for review March 18, 2002)

The impact of nitric oxide (NO) synthesis on different biological cascades can rapidly change dependent on the rate of NO formation and composition of the surrounding milieu. With this perspective, we used diaminonaphthalene (DAN) and diaminofluorescein (DAF) to examine the nitrosative chemistry derived from NO and superoxide (O_2^-) simultaneously generated at nanomolar to low micromolar per minute rates by spermine/NO decomposition and xanthine oxidase-catalyzed oxidation of hypoxanthine, respectively. Fluorescent triazole product formation from DAN and DAF increased as the ratio of O_2^- to NO approached equimolar, then decreased precipitously as O_2^- exceeded NO. This pattern was also evident in DAF-loaded MCF-7 carcinoma cells and when stimulated macrophages were used as the NO source. Cyclic voltammetry analysis and inhibition studies by using the N_2O_3 scavenger azide indicated that DAN- and DAF-triazole could be derived from both oxidative nitrosylation (e.g., DAF radical + NO) and nitrosation (NO^+ addition). The latter mechanism predominated with higher rates of NO formation relative to O_2^-. The effects of oxymyoglobin, superoxide dismutase, and carbon dioxide were examined as potential modulators of reactant availability for the O_2^- + NO pathway *in vivo*. The findings suggest that the outcome of NO biosynthesis in a scavenger milieu can be focused by O_2^- toward formation of NO adducts on nucleophilic residues (e.g., amines, thiols, hydroxyl) through convergent mechanisms involving the intermediacy of nitrogen dioxide. These modifications may be favored in microenvironments where the rate of O_2^- production is temporally and spatially contemporaneous with nitric oxide synthase activity, but not in excess of NO generation.

Biosynthesis of nitrogen monoxide (NO) from nitric-oxide synthase (NOS)-catalyzed oxidation of L-arginine can lead to selective formation of NO adducts on protein residues, which modulates homeostatic metabolism and affects numerous pathophysiologic responses. *N*-nitrosamines and *S*-nitrosothiols are typically formed via donation of a nitrosonium equivalent (NO^+) from dinitrogen trioxide (N_2O_3) to the nucleophilic residue (1). The function of many proteins has been altered by nitrosation *in vitro* including caspases (2, 3), glyceraldehyde-3-phosphate dehydrogenase (4), the *N*-methyl-D-aspartate receptor (5, 6), O^6-methylguanine-DNA-methyltransferase (7, 8), ras (9) and the ryanodine receptor (10).

The mechanism through which these modifications may occur in biological systems is a subject of debate. Many have questioned the relevance of nitrosation via NO autoxidation, reasoning that sufficient levels of NO cannot be achieved *in vivo* to satisfy the rate-limiting step for N_2O_3 formation, which is second order in NO (11–20). In contrast to NO autoxidation, the reaction between NO and superoxide (O_2^-) is first order in both reactants and occurs at near diffusion control (21–24). Much emphasis has been placed on the product of this reaction, peroxynitrite ($ONOO^-$), as an important mediator of oxidation and nitration (23–28). In this study, we tested the hypothesis that $ONOO^-$ may also serve as an intermediary in a pathway leading to formation of NO adducts (e.g., *N*-nitrosamines, *S*-nitrosothiols) *in vivo*. The results suggest that these moieties may be produced through both nitrosation and oxidative nitrosylation dependent mechanisms, which are strongly influenced by the relative rates of NO and O_2^- formation.

Methods

Generation of O_2^- and NO. Formation of O_2^- from conversion of hypoxanthine (HX, 500 μM; Sigma) to xanthine was catalyzed by xanthine oxidase (XO; Roche; ref. 29) in PBS (pH 7.4, 37°C) containing the metal chelator diethylenetriaminepentaacetic acid (DTPA, 50 μM; Sigma). The rate of O_2^- formation by stock enzyme was assessed by cytochrome *c* reduction (Sigma; 570 nm, ε = 21,000 $M^{-1}\cdot cm^{-1}$; ref. 30). NO was produced by decomposition of spermine/NO (a generous gift from J. A. Hrabie, National Cancer Institute-Frederick Cancer Research and Development Center, Frederick, MD; ref. 31). Buffer pH (7.4) and temperature (37°C) were confirmed before each experiment because of the major influence these parameters have on the rate of spermine/NO decomposition ($t_{1/2}$ = 42 min). Rates of NO release were determined by measuring oxymyoglobin oxidation (582 nm, ε = 9,100 $M^{-1}\cdot cm^{-1}$) in PBS solution containing DTPA and HX (HX buffer, ref. 32). Oxymyoglobin was prepared by reducing myoglobin (500 μM; Sigma) in water with excess sodium dithionite (Fluka) followed by passage through a Sephadex G-25 column (PD-10; Amersham Pharmacia). Steady-state NO concentrations were also assessed by using a NO selective electrode (World Precision Instruments, Sarasota, FL) controlled by a DUO18 amplifier. Peak amplitude was calibrated by using standard curves generated with argon-purged PBS solutions of saturated NO (Matheson) after determination of NO concentration with 2-2′-azinobis(3-ethylbenzthiazoline-6-sulfonic acid) (660 nm, ε = 12,000 $M^{-1}\cdot cm^{-1}$; Sigma; refs. 32 and 33). Murine ANA-1 macrophages were stimulated to generate NO by treatment overnight with IFN-γ (100 units/ml; R&D Systems) followed by 4 h incubation with lipopolysaccharide (LPS; *E. coli*, 0111:B4; Sigma; ref. 34).

Experimental Paradigms. Assays were conducted in either black microtiter plates (200 μl, nonstirring; Dynex, Manasas, VA) or fluorometric cuvettes (2 ml, stirring; Spectrocell, Oreland, PA) containing XO in HX buffer and either 2,3-diaminonaphthalene (DAN; Fluka), 4,5-diaminofluorescence (DAF, Calbiochem) with copper/zinc superoxide dismutase (SOD, Sigma) or oxymyoglobin (Sigma) as indicated. Sodium azide (Sigma) concentration was 1 mM.

Experiments commenced upon addition of spermine/NO, with the exception of macrophage experiments, where XO was added secondary to equilibration of cells into HX buffer (pH 7.4, 37°C) supplemented with L-arginine (1 mM, Sigma) and D-glucose (20

This paper was submitted directly (Track II) to the PNAS office.

Abbreviations: NOS, nitric-oxide synthase; iNOS, inducible NOS; HX, hypoxanthine; XO, xanthine oxidase; DTPA, diethylenetriaminepentaacetic acid; DAN, diaminonaphthalene; DAF, diaminofluorescein; NHE, normal hydrogen electrode; SOD, superoxide dismutase.

*To whom reprint requests should be addressed at: Radiation Biology Branch, National Cancer Institute, National Institutes of Health, Building 10, Room B3-B69, Bethesda, MD 20892. E-mail: sp@nih.gov.

BIOCHEMISTRY

mM, Sigma). For CO_2 experiments, 25 mM $NaHCO_3$ was added to the buffer (final pH 7.4), and the reaction was carried out in an atmosphere of 5% CO_2, 95% air. Incubation times were 1 h at 37°C unless otherwise indicated. Intracellular triazole formation was examined with 85–90% confluent adherent human MCF-7 breast carcinoma cells [American Type Culture Collection (ATCC), Manassas, VA] incubated with RPMI media 1640 containing DAF diacetate (5 μM; Calbiochem) in black-wall microtiter plates for 30 min. After several washes with PBS solution, the cells were gently covered with HX buffer (200 μl, pH 7.4) supplemented with D-glucose (20 mM) and then were exposed to spermine/NO and XO while maintained at 37°C in an atmosphere of 5% CO_2, 95% air. Intracellular DAF was of sufficient quantity to detect nitrosation at NO concentrations ≥100-fold the maximum concentration used (35). End-point MCF-7 viability, assessed by trypan blue dye exclusion, was found to be >95% (35). DAF fluorescence in the supernatant was <2% of the total, indicating that DAF release from cells under experimental conditions was negligible.

Spectroscopy. UV-visible spectroscopy was performed with a Hewlett–Packard 8452A diode-array spectrophotometer. Fluorescence measurements were obtained on either a Perkin-Elmer HTS 7100 plate reader or an LS50B fluorometer. Formation of the fluorescent products DAN- and DAF-triazole was linear from 15–90 min (data not shown). The fluorescent products from DAN and DAF derived from either NO autoxidation or the NO + O_2^- paradigms had identical fluorescent excitation and emission spectra (data not shown).

Cyclic Voltammetry. Cyclic voltammetry was performed with an EG & G Princeton Applied Research potentiostat/galvanostat (273/PAR 270 software). The working electrode was a glassy carbon disk with a Pt counter electrode and Ag/AgCl reference electrode [+0.222 V vs. normal hydrogen electrode (NHE)]. Compounds were examined from 0 to +1.8 V at a rate of 100 mV/s in acetonitrile (Baker) containing tetraethylammonium perchlorate (0.1 M, Fluka) as the electrolyte. The electrode surface was cleaned between runs because of interference from electroplating, which contributed to the lack of signal reversibility. Fluoresceinamine (AF; Sigma) and 5,6-carboxyfluorescein (CF; Molecular Probes) served as fluorescein derivative controls.

Results

Reactions with DAN. N-nitrosation of DAN results in the formation of fluorescent product 2,3-naphthotriazole (DAN-triazole; refs. 34 and 36). Consistent with previous experimental findings on aqueous NO autoxidation, decomposition of spermine/NO (6 μM, ≈140 nM NO/min) in HX buffer containing DAN resulted in formation of DAN-triazole (Fig. 1, 0 O_2^-). Addition of XO to this system augmented fluorescence incrementally, with maximal signal observed at an XO activity of 60 nM/min O_2^-, which was ≈175% relative to spermine/NO alone. At higher XO activities, DAN-triazole fluorescence decreased markedly, with complete quenching at ≥1 μM O_2^-/min. XO alone did not result in an increase in fluorescence above background (data not shown).

Double reciprocal plots of DAN-triazole fluorescence as a function of DAN concentration (Fig. 4, which is published as supporting information on the PNAS web site, www.pnas.org) indicate that the species produced by NO autoxidation and by the NO + O_2^- reactions have different affinities for DAN. The $-X_{int}^{-1}$ is an indication of the relative reactivity of species formed by either pathway. Exposure to spermine/NO (6 μM, ≈140 nM NO/min; 90 min) resulted in a $-X_{int}^{-1}$ of 95 ± 15 μM, whereas addition of 125 nM O_2^-/min decreased the $-X_{int}^{-1}$ to 62 ± 12 μM. At infinite concentrations of DAN, the projected maximal fluorescence values (Y_{int}^{-1}) were similar, indicating that the maximal amounts of reactive species formed were comparable. The difference in relative reactivity for DAN ($-X_{int}^{-1}$) suggests distinct mechanisms for DAN-triazole formation via NO autoxidation and a NO + O_2^- reaction pathway.

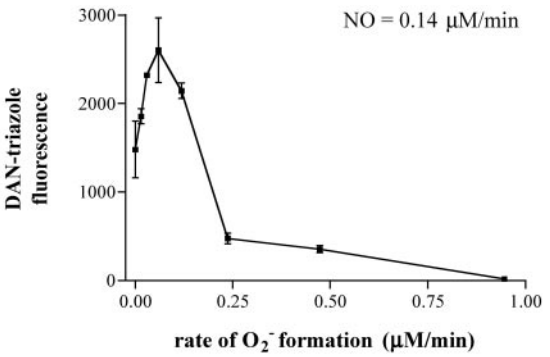

Fig. 1. Reacitivy of DAN with NO + O_2^-. Reactions were carried out in HX buffer as described in *Methods* containing DAN (30 μM) and XO to give the indicated O_2^- flux for 1 h after the addition of spermine/NO (6 μM). Shown are representative data (n = three trials) of fluorescence (triplicate mean ± SEM) monitored at $\lambda_{ex/em}$ of 360/465 nm (gain 75) minus background.

Reactions with DAF. Studies have shown that N-nitrosation of DAF results in formation of fluorescent 4,5-naphthotriazole (DAF-triazole; refs. 35 and 37). NO generated in tandem with varied rates of O_2^- resulted in DAF-triazole fluorescence changes that were similar to those observed with DAN (data not shown). DAF-triazole formation as a function of NO at several different rates of O_2^- formation is shown in Fig. 2*A*. The enhancement of this signal in the presence of O_2^- vs. NO alone (NO autoxidation) was determined by subtracting the fluorescence values derived from NO in the absence of O_2^- (Fig. 2*A*, open symbols) from values obtained with simultaneous NO and O_2^- production (solid symbols). The actual data are a combination of these values (open symbols + solid symbols). Doubling O_2^- formation increased the fluorescence maxima in a staircase pattern. For each data set, peaks occurred at points where the rate of O_2^- formation approached the rate of NO production, then decreased as the rate of O_2^- formation exceeded that of NO.

Macrophages stimulated to express inducible NOS (iNOS) with IFN-γ and lipopolysaccharide (LPS) have been shown to elicit nitrosative reactions (34). We examined whether XO-catalyzed formation of O_2^- influences macrophage-mediated reactivity with DAF in solution (Fig. 2*B*). The burst of DAF-triazole formation visible immediately after addition of XO may be attributed to O_2^- reacting with the steady-state concentration of NO available in the cuvette. Within minutes, a new ratio between NO generated by iNOS and each concentration of XO-derived O_2^- could be distinguished as varying rates of fluorescence production. Analogous to the pattern observed by using the synthetic NO source spermine/NO, a bell-shaped concentration dependence for O_2^- in macrophage-mediated augmentation of DAF-triazole formation was evident.

To determine how simultaneously generated O_2^- and NO and their subsequent reaction products interact with the complex milieu of viable cells, MCF-7 carcinoma cells were incubated with DAF-diacetate, which was taken up from the media and retained as DAF in the cytoplasm after esterase-mediated cleavage (35). A 2- to 4-fold increase in the concentrations of both O_2^- and NO was required to achieve a relative fluorescence signal inside cells comparable to that observed with DAF in buffer (Fig. 2*C*). Important issues to consider when comparing reactions in homogeneous buffer to a heterogeneous cellular system are fluorophore compartmentalization and cellular consumptive processes that do not exist in buffer. The shape of profiles derived from intracellular DAF closely resembled those generated with either DAN or DAF

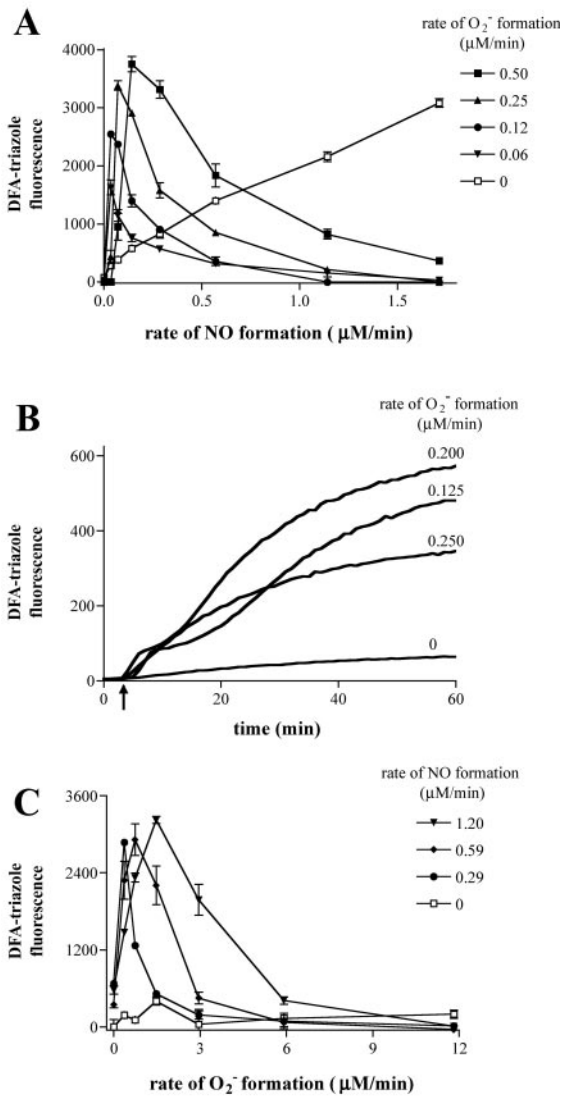

Fig. 2. Reacitivy of DAF with NO + O_2^-. (*A*) XO was added to HX buffer containing DAF (1 μM) to give O_2^- flux as indicated. Spermine/NO was subsequently added forming NO as indicated. Shown are representative data (triplicate mean ± SEM, n = three trials) of fluorescence monitored at $\lambda_{ex/em}$ of 485/535 nm (gain = 75) after 1 h incubation at 37°C. Fluorescence values obtained with spermine/NO in the absence of XO (□) have been subtracted from the data acquired in the presence of XO (filled symbols). (*B*) ANA-1 murine macrophages (1×10^6) stimulated to express iNOS as described in *Methods*. Arrow indicates time of XO addition to HX buffer to give O_2^- flux as indicated. (*C*) XO was added to HX buffer covering adherent MCF-7 cells loaded with DAF-diacetate as described in *Methods* to give the indicated O_2^- fluxes. Fluorescence values were obtained (as in *A*) 1 h after addition of spermine/NO to give the indicated NO fluxes.

in buffer (e.g., Fig. 1). Peak intracellular DAF-triazole fluorescence was augmented ≈4- to 5-fold by the combination of O_2^- and NO relative to the signal generated from NO autoxidation in the absence of O_2^-.

Specificity of Diamine Fluorophores for Nitrosation. We and others have observed that DAF has the potential to yield fluorescent product after exposure to nitrogen oxide oxidants (38, †). The ability of DAF and DAN to donate electrons was measured by cyclic voltammetry vs. Ag/AgCl (Fig. 5*A*, which is published as supporting information on the PNAS web site). These data show that the oxidation potential for DAN is 0.88 V (1.11 V vs. NHE), whereas DAF is oxidized between 0.85 to 1.25 V (1.07 to 1.47 V vs. NHE). Fluoresceinamine has a single oxidation potential of 1.2 V (1.42 V vs. NHE), whereas 5,6-carboxyfluorescein was essentially resistant to oxidation ($E > 2.0$ V; 2.2 V vs. NHE), suggesting that oxidation was localized to the amino moieties of DAF with some facilitation by the fluorescein ring. Under these conditions, an oxidation potential of 1.0 V (1.22 V vs. NHE) was observed with dihydrorhodamine, a commonly used indicator of oxidation (data not shown). These data suggest that oxidation of DAN and DAF may be feasible under biological conditions.

The contribution of N_2O_3 to DAN-triazole and DAF-triazole formation was assessed by azide scavenging studies (12). Addition of azide subsequent to triazole formation did not affect fluorescence (data not shown). Azide (1 mM) quenched >90% of DAN-triazole formation (30 to 200 μM DAN) during NO autoxidation derived from relatively high concentrations of NO (≥50 μM spermine/NO, ≥1.2 μM NO/min; Fig. 5*B*). The combination of XO (125 nM O_2^-/min) and spermine/NO (6 μM, 140 nM/min) was tested in the presence and absence of azide to determine the level of nitrosation via N_2O_3 at the optimal ratio of O_2^- to NO for maximal fluorescent product formation. Under these conditions, the presence of azide inhibited DAN- and DAF-triazole formation 23 ± 5% and 18 ± 3%, respectively (Fig. 5*B*). These data indicate that ≈20% of the fluorescence signal derived from the diamine fluorophores at low nM per minute rates of simultaneous O_2^- and NO generation was due to N_2O_3.

Modulators of the O_2^- + NO Reaction. The influence of several biologically relevant scavengers for O_2^-, NO, and their related species on nitrosation was examined by using DAF as an indicator. The ubiquitous metabolic by-product CO_2 can readily react with $ONOO^-$ (39–44). The effect of CO_2 on DAF-triazole formation by simultaneous production of O_2^- (varied XO) and NO (spermine/NO 3 μM, ≈70 nM NO/min) is shown in Fig. 3*A*. Reaction in buffer equilibrated with CO_2 at physiologic concentration resulted in an approximate 2-fold increase in fluorescence maximum. The effect was lessened with each point away from the peak.

The capacity of the O_2^- + NO pathway to form DAF-triazole in the presence of oxymyoglobin is shown in Fig. 3*B*. Initial experiments showed that addition of 10 μM oxymyoglobin to DAF-triazole (1 μM) decreased fluorescence 23% because of an interference filter effect (data not shown). Although quenching was significant, sufficient fluorescence formation was observed under the assay conditions to allow real-time analysis. The presence of 10 μM oxymyoglobin was adequate to competitively scavenge NO (4 μM spermine/NO, ≈90 nM NO/min) evidenced by a lack of fluorescence production from DAF. Under these conditions, an emergence of fluorescence was observed on introduction of O_2^- generated by XO/HX at a rate of 2 μM/min. These results indicate that this level of O_2^- was sufficient to outcompete oxymyoglobin for reaction with NO subsequently leading to DAF-triazole formation.

Superoxide dismutase (SOD), which catalytically converts O_2^- to hydrogen peroxide (30, 45), did not significantly effect DAF-triazole formation via NO autoxidation during decomposition of spermine/NO (6 μM, ≈140 nM NO/min; data not shown). In contrast, relatively small amounts of SOD (≥3.1 μg/ml; equivalent to ≈10 units/ml) significantly influenced the development of DAF-triazole fluorescence by this level of NO when produced in combination with O_2^- (Fig. 3*C*). The presence of SOD shifted the initial peak for fluorescence to a higher O_2^- rate, indicating that a 2-fold greater concentration of O_2^- was required to achieve a comparable initial level of DAF-triazole formation. In addition, SOD broadened the range of XO concentrations in which DAF-triazole was formed in a dose-dependent fashion. The highest level of SOD tested (25 μg/ml) increased DAF-triazole production

†Jourd'heuil, D. (2001) *Free Radical Biol. Med.* **31,** S80 (abstr.).

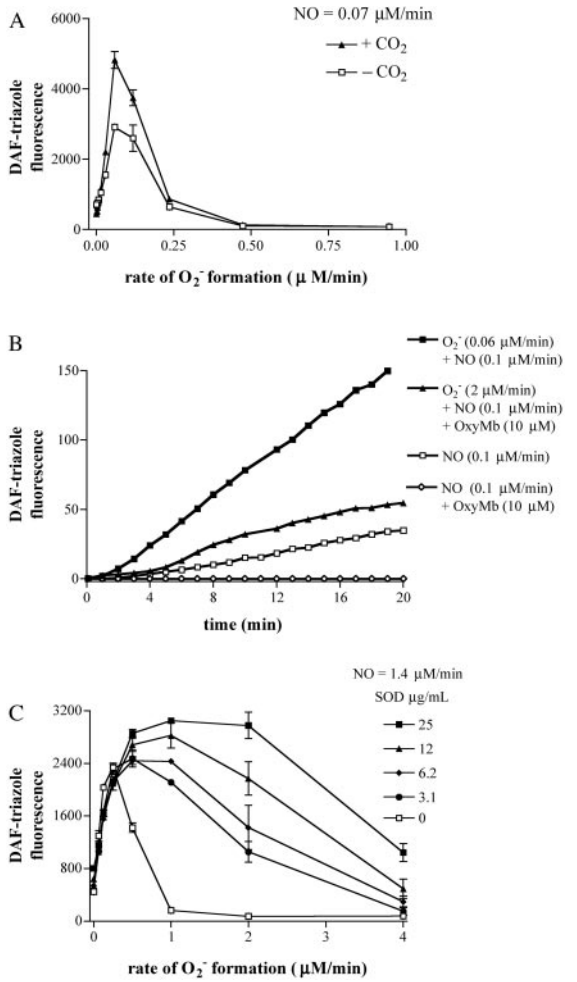

Fig. 3. Modulators of NO + O_2^- reaction. (*A*) Spermine/NO (3 μM) was added to HX buffer containing DAF (1 μM) and XO to give O_2^- flux as indicated in either the presence (▲) or absence (□) of 25 mM $NaHCO_3$ with a 5% CO_2, 95% air atmosphere. Fluorescence was measured ($\lambda_{ex/em}$ of 485/535 nm) after incubation at 37°C for 1 h. (*B*) DAF-triazole formation was monitored (as in *A*) in HX buffer containing DAF (1 μM) under conditions as indicated. (*C*) Spermine/NO (6 μM) was added to HX buffer containing DAF (1 μM) and XO to give O_2^- flux as indicated in the presence of SOD as indicated. Fluorescence was measured (as in *A*) after incubation at 37°C for 1 h.

derived from spermine/NO (140 nM NO/min) and XO (1 μM O_2^-/min) over 17-fold. Inclusion of azide under these conditions quenched DAF-triazole formation ≈12% (data not shown), suggesting a limited, but measurable, contribution from N_2O_3. Experiments conducted with both SOD and catalase showed a decrease in DAF-triazole formation only when catalase levels were sufficient to competitively react with NO to form a stable a catalase-nitrosylheme complex, thereby altering the NO balance with O_2^- (data not shown). This finding suggests that H_2O_2 was inconsequential under our experimental conditions.

Discussion

XO in conjunction with synthetic and macrophage iNOS sources of NO has been used as a model to study the O_2^-/NO reaction. Beyond this simple system, XO-mediated generation of O_2^- through purine catalysis plays a role in inflammatory or ischemia and reperfusion injury (46, 47). During these events, XO from distal sources can be enriched on endothelial cell surfaces or the interstitial matrix by binding glycosaminoglycan residues, which can result in aberrant O_2^- formation at these sites (48, 49). These conditions can also elicit changes in NO formation from the various NOS isoforms expressed by the endothelia, associated neurons, and resident or recruited immune cells, thereby altering the dynamic for NO participation in signaling cascades.

The rapid reaction between O_2^- and NO (21–24) has prompted numerous investigators to focus on $ONOO^-$ and the roles it may play in oxidation and nitration of susceptible molecules (23–28). Data have been largely lacking, however, on whether the putative damage elicited by $ONOO^-$ may be modulated or counteracted by the additional reactions of $ONOO^-$ occurring when NO is produced at a variable rate compared with O_2^-. Therefore, we examined the potential for nitrosation during simultaneous, but varied generation of O_2^- and NO under conditions relevant to their formation at basal levels (nanomolar) and levels that may disrupt regulatory processes (low micromolar).

A characteristic reaction pattern based on relative O_2^- and NO fluxes was evident in experiments with the N-nitrosation indicators (34–37) DAN (Fig. 1) and DAF (Fig. 2). In both cases, product formation was maximal when the ratio of O_2^- to NO was nearly equivalent, but with NO still in slight excess. These findings were consistent with studies that have shown that the balance between O_2^- and NO rates of formation is a critical determinant in the type of chemistries they bring to bear. Under conditions of intracellular O_2^- formation from menadione and mitomycin C redox cycling within tumor cells, subtle increases in NO exposure (from 250–500 nM/min) resulted in switching from amplification of dihydrorhodamine oxidation to abatement (50). These data were consistent with the patterns of dihydrorhodamine oxidation observed in solution during covariation of NO and O_2^- rates of formation (44, 51). Activity measurements from purified alcohol dehydrogenase after incubation with XO/HX and spermine/NO showed that inhibitory oxidation was maximal at a correspondence between NO and O_2^- rates of formation (52). Relief of inhibition in favor of nitrosative chemistry was observed as NO was increased ≥2-fold relative to O_2^-. The importance of stoichiometry between O_2^- and NO has also been noted in the oxidation of lipids (53), hydroxylation of benzoate (51), nitration of tyrosine (54) and various peptides (unpublished observation) as well as in the formation of disulfides vs. *S*-nitrosothiols (refs. 55–57; X. Wang, M. T. Gladwin, and M.G.E., unpublished observation). These examples typify how contemporaneous production of O_2^- and NO may result in a variety of functional outcomes dependent on their relative rates of formation, the target characteristics, and the composition of the surrounding milieu.

The pivotal importance of balance in the biochemistry of O_2^- and NO generation cannot be fully appreciated in experimental paradigms that use bolus application of synthetic $ONOO^-$. Peroxynitrite anion can be protonated to form peroxynitrous acid (ONOOH, pK_a = 6.8; ref. 23). NO can react with intermediates formed in the decomposition of $ONOO^-$/ONOOH in either the absence or presence of CO_2 (44, 55). Although these reactions generally lead to an abatement of oxidation, nitrosation reactions can still occur under conditions of excess NO via formation of N_2O_3 (Eq. **1**–**3**).

$$ONOOH + NO \rightarrow NO_2 + NO_2^- + H^+ \quad [1]$$

$$ONOO^- + CO_2 + NO + H_2O \rightarrow NO_2 + NO_2^- + CO_3^{2-} + 2H^+ \quad [2]$$

$$NO_2 + NO \leftrightarrow N_2O_3 \quad [3]$$

DAF was chosen as a probe of N-nitrosation for its sensitivity and ability to be sequestered within cells (35, 37). However, we and others[†] have observed that DAF-triazole formation is not strictly related to reaction with N_2O_3. Cyclic voltammetry analysis indicated that the oxidation potentials of DAF and DAN are

in the range of 0.85–1.2 V (Fig. 5*A*; 1.07 to 1.42 V vs. NHE) suggesting the possibility of an oxidative pathway for nitrosation rather than addition of nitrosonium by N_2O_3. At the ratio of O_2^- to NO required for optimal fluorescent product formation from either DAN or DAF, inclusion of the specific N_2O_3 scavenger azide (12) resulted in only ≈20% inhibition of triazole generation (Fig. 5*B*). These data signify that triazole product may be formed predominantly by oxidative nitrosylation under these conditions, a process that involves oxidation of the compound followed by direct reaction with NO (Eqs. **4** and **5**; refs. 58 and 59).

$$XH \xrightarrow{-e^-} X^{+\bullet} + H^+ \quad [4]$$

$$X^{+\bullet} + NO \rightarrow XNO \quad [5]$$

From a mechanistic viewpoint, the reactions of $DAN^{+\bullet}$ and $DAF^{+\bullet}$ intermediates with NO must be competitive with respect to a variety of reactive species produced during simultaneous generation of O_2^- and NO. Of note, azide inhibition studies indicated that oxidative nitrosylation did not completely preclude nitrosation via N_2O_3 (Eq. **6**) during O_2^- and NO cogeneration, despite only nanomolar rates of NO formation in our system (Fig. 5*B*).

$$XH + N_2O_3 \rightarrow XNO + H^+ + NO_2^- \quad [6]$$

This observation suggests that, during the 1-h experimental time frame, a small portion of NO could react by Eq. **1–3** to form N_2O_3 despite competing with the reaction in Eq. **5**.

From these observations, it becomes evident that formation of nitrosated triazole complexes can be produced by either nitrosation (intermediacy of N_2O_3) or through oxidative nitrosylation. The factors that determine which pathway leads to formation of nitrosated product include differences in relative rates of O_2^- and NO formation and qualities inherent to the substrate nucleophilicity, oxidation potential, residue location, and interaction with metals. Daiber *et al*. exposed phenol to relatively high levels of NO (spermine/NO, 100 μM) in combination with SIN-1 (200 μM), which simultaneously decomposes to NO and O_2^-, and observed that azide inhibited 4-nitrosophenol formation by 64% (52). This finding suggests that, under these conditions (25), nitrosation of phenol proceeded mostly through nitrosation rather than oxidative nitrosylation. These data support earlier studies that suggest that a susceptibility hierarchy of amine, hydroxyl, and thiol constituents likely exist for formation of NO adducts *in vivo* (12, 25, 35, 51, 55).

An important observation in this study was that the pattern of DAF-triazole formation in solution was comparable to that within intact cells (Fig. 2*A* and *C*). These data suggest formation of similar reactive intermediates, which may readily cross the plasma membrane. Data showing incomplete inhibition by azide coupled with the relatively high oxidation potentials observed for DAN and DAF (Fig. 5*A*) indicate formation of a reactive intermediate capable of transmembrane diffusion during simultaneous O_2^- and NO generation. On the basis of the near diffusion control rate constant for the O_2^- + NO reaction (21–24) and the relative membrane impermeability of O_2^- ($pK_a = 4.8$; refs. 30 and 45), the ingressive species most likely is a reactive nitrogen oxide. Under our experimental conditions, initial formation of $ONOO^-$ on the outside of the cell is predicted (21–24). Once protonated, this species can decompose leading to secondary formation of other oxidants, chiefly NO_2 and hydroxyl radical ($^\bullet OH$; refs. 21, 23, and 60–62). It is unlikely that the highly reactive $^\bullet OH$ molecule would have sufficient lifetime for diffusion into the cell. A more likely candidate is NO_2, a sufficient oxidant (63) that can be produced via Eqs. **1** and **2** that is capable of permeating cells (35, 40, 50) for reactivity with cytoplasmic DAF (35).

An important facet to consider in the biochemistry of NO and O_2^- is the influence of CO_2 on this system. Reports on the ingress of $ONOO^-$/ONOOH into cells (41, 64) suggest that these species could potentially react with intracellular DAF. Cell experiments were performed under standard culture conditions in which buffer was equilibrated with physiologic CO_2 levels. Several groups have demonstrated that $ONOO^-$ can be rapidly consumed by CO_2 to form the CO_2 adduct nitrosoperoxocarbonate ($ONOOCO_2^-$; refs. 39–44). This reaction pathway would decrease the lifetime, thus diffusion distance of $ONOO^-$ circumventing the putative homolysis of ONOOH to NO_2 and $^\bullet OH$ in favor of $ONOOCO_2^-$ decomposition into NO_2 and carbonate radical ($CO_3^{\bullet -}$; Eqs. **7** and **8**).

$$ONOO^- + CO_2 \rightarrow ONOOCO_2^- \quad [7]$$

$$ONOOCO_2^- \rightarrow NO_2 + CO_3^{\bullet -} \quad [8]$$

In our cell-free system, CO_2 slightly enhanced peak DAF-triazole formation (2-fold, Fig. 3*A*), but did not alter the overall NO to O_2^- relationship, suggesting that the CO_2 reaction pathway may result in a modestly enhanced level of NO_2 formation relative to that produced by alternate routes of $ONOO^-$ catabolism. Taken together with the intracellular DAF results, these data argue against $ONOO^-$, ONOOH or $ONOOCO_2^-$ as a significant cell permeable species relative to NO_2 (39, 49).

In vivo, CO_2 may modulate NO_2 formation through the intermediacy of $ONOOCO_2^-$ during contemporaneous NO and O_2^- generation, resulting in selective and focal zones of oxidation, nitration, and nitrosation/oxidative nitrosylation dependent on the inter- and intracellular compartmentalization of the target substrate (40, 43, 44, 49, 50, 64). Oxidation of dihydrorhodamine by either the $ONOO^-$/ONOOH or $ONOOCO_2^-$ route in aqueous solution was found to be comparable (44). An elegant study by the Kalyanaraman group showed that $ONOO^-$ exposure in the presence of CO_2 augmented oxidation and nitration of a tyrosine probe in solution, but did not enhance these reactions in membranes (43). Using vesicular-trapped $Fe(CN)_6^{3-}$, Hurst and colleagues showed that, in the presence of CO_2, the vast majority of extracellular ONOOH was converted via the intermediacy of $ONOOCO_2^-$ to NO_2 before transmembrane diffusion could occur (40). The commonality of NO_2 as a putative product of the ONOOH or $ONOOCO_2^-$ decomposition pathways in combination with the ability of NO_2 to diffuse into cells and mediate oxidation (40, 49) suggest it to be a key intermediary in the process of NO adduct formation via the oxidative nitrosylation pathway. The findings advocate that CO_2 would not block formation of NO adducts under physiologic conditions (65) and suggest how O_2^- may facilitate this process.

We observed that DAN had a greater affinity for the reactive species formed by the O_2^- + NO pathway relative to that produced during NO autoxidation (Fig. 4). This finding was consistent with our earlier analysis of DAF, which showed similar differences in relative reactivity of species produced by NO + NO_2 vs. aqueous NO autoxidation (35). We promote the viewpoint that the cell may provide an environment, such as within membranes (66), that is favorable for NO autoxidation to produce NO_2 (35) and in the current study suggest that NO_2 formation through the intermediacy of $ONOO^-$ is a key agent leading to formation of NO adducts on biological molecules. An examination of nitration-induced quenching of green fluorescent protein within cells showed that heme-peroxidase-catalyzed oxidation of nitrite was a more effective generator of NO_2 than balanced NO and O_2^- generation (50). These data suggest that the presence of peroxidase and H_2O_2 may also affect formation of NO adducts through the intermediacy of NO_2 when present in conjunction with NOS activity.

Regardless of the reactive intermediates involved, the pathways for generation of NO adducts differ in the context of the relative rate of NO formation and the presence of O_2^-, which may form the basis for divergent reaction mechanisms and functional outcomes

from NOS activity. Nitrosation via NO autoxidation may be the dominant route when relatively high rates of NO formation occur under aerobic conditions without significant O_2^- generation, which would favor nitrosation through N_2O_3 formation subsequent to reaction of NO_2 with an additional NO molecule (Eq. **3**; Scheme 1, which is published as supporting information on the PNAS web site; refs. 11–20, 35, 36, and 66). Triazole formation (e.g., Fig. 5*A*) and azide inhibition studies (Fig. 5*B*) showed that >600 nM NO/min (spermine/NO 24 μM) was sufficient to foster significant formation of the nitrosating species N_2O_3 (<250 nM O_2^-/min). This condition may be most applicable to recruitment of immune cells expressing iNOS to sites either spatially or temporally dissociated from O_2^- sources, for instance during inflammatory events secondary to the acute phase response.

In contrast, oxidative nitrosylation and nitrosation mediated by an $ONOO^-$ derived NO_2 pathway (Eqs. **1-3**) may chiefly prevail under conditions where O_2^- was present, but not in great excess of NO. Basal formation of nitrosated compounds may for the most part occur on a subtle scale, in discrete zones that favor such equivalence between nanomolar levels of O_2^- and NO by virtue of their reactivity with each other vs. consumption by respective scavenger substances and competing reactions. This result was illustrated in Fig. 3*B*, where the addition of sufficient O_2^- successfully diverted NO from reaction with oxymyglobin toward $ONOO^-$ formation and subsequent reactions to promote DAF-triazole generation. SOD in our system consumed excess O_2^- with respect to NO, thereby maintaining the appropriate alignment between O_2^- and NO rates, effectively augmenting reactivity with DAF over a broader range of O_2^- (Fig. 3*C*; refs. 54 and 67). The intermediacy of $ONOO^-$ in the formation of NO adducts on nucleophiles may be a relevant regulatory mechanism where simultaneous, but low-level, generation of both O_2^- and NO may episodically occur; for instance, membrane proteins on leukocyte and endothelial cell surfaces (68, 69) and within organelles such as mitochondria (3, 70).

This process may affect a different set of signal cascades if high levels of O_2^- and NO are produced in tandem. Fig. 2 *A* and *C* shows that a balanced spatial and temporal relationship between of O_2^- and NO may focus this chemistry, typified by a staircase pattern for peak formation of DAF-triazole as each set of increased rates of O_2^- and NO came into concordance. In lesion sites involving XO deposition and leukocytic infiltration under pathological conditions, for instance, higher rates of O_2^- and NO formation may coincide accordingly to foster a greater magnitude and duration of oxidative nitrosylation/nitrosation, a possibility supported by the ability of stimulated macrophages to produce this chemistry during XO catalysis of hypoxanthine (Fig. 2*B*). Under pathogenic conditions, formation of NO adducts via these oxidative nitrosylation and nitrosation mechanisms may serve to abate and resolve deleterious actions derived from $ONOO^-$ formation (<2 NO to 1 O_2^-) such as oxidation (refs. 53, 55, and 68–72; Scheme 1).

In summary, this study suggests that small differences in the location and rates of O_2^- and NO generation *in vivo* will have a dramatic influence on the ultimate functional outcomes these species mediate. In a biological system, these factors are constantly changing. Therefore, the sphere of influence for a particular chemistry resulting from NO biosynthesis (e.g., oxidation, nitration, oxidative nitrosylation, nitrosation) may be delineated and dynamically focused by O_2^-.

1. Williams, D. L. H. (1988) *Nitrosation* (Cambridge Univ. Press, Cambridge, U.K.).
2. Rossig, L., Fichtlscherer, B., Breitschopf, K., Haendeler, J., Zeiher, A. M., Mulsch, A. & Dimmeler, S. (1999) *J. Biol. Chem.* **274,** 6823–6826.
3. Mannick, J. B., Schonhoff, C., Papeta, N., Ghafourifar, P., Szibor, M., Fang, K. & Gaston, B. (2001) *J. Cell Biol.* **154,** 1111–1116.
4. Molina y Vedia, L., McDonald, B., Reep, B., Brune, B., DiSilvio, M., Billiar, T. R. & Lapetina, E. G. (1992) *J. Biol. Chem.* **267,** 24929–24932.
5. Gbadegesin, M., Vicini, S., Hewett, S. J., Wink, D. A., Espey, M., Pluta, R. M. & Colton, C. A. (1999) *Am. J. Physiol.* **277,** C673–C683.
6. Espey, M. G., Colton, C. A., Pluta, R. M., Miranda, K. M., Hewett, S. J. & Wink, D. A. (2000) *Free Radicals in Brain Pathophysiology* (Dekker, New York), pp. 523–540.
7. Laval, F. & Wink, D. A. (1994) *Carcinogenesis* **15,** 443–447.
8. Wink, D. A. & Laval, J. (1994) *Carcinogenesis* **15,** 2125–2129.
9. Lander, H. M., Hajjar, D. P., Hempstead, B. L., Mirza, U. A., Chait, B. T., Campbell, S. & Quilliam, L. A. (1997) *J. Biol. Chem.* **272,** 4323–4326.
10. Sun, J., Xin, C., Eu, J. P., Stamler, J. S. & Meissner, G. (2001) *Proc. Natl. Acad. Sci. USA* **98,** 11158–11162.
11. Wink, D. A., Darbyshire, J. F., Nims, R. W., Saavedra, J. E. & Ford, P. C. (1993) *Chem. Res. Toxicol.* **6,** 23–27.
12. Wink, D. A., Nims, R. W., Darbyshire, J. F., Christodoulou, D., Hanbauer, I., Cox, G. W., Laval, F., Laval, J., Cook, J. A., Krishna, M. C., *et al.* (1994) *Chem. Res. Toxicol.* **7,** 519–525
13. Wink, D. A., Ford, P. C. & Stanbury, D. M. (1993) *FEBS Lett.* **326,** 1–3.
14. Fukuto, J. (1995) *Adv. Pharmacol.* **34,** 1–15.
15. Lewis, R. S. & Dean, W. M. (1994) *Chem. Res. Toxicol.* **7,** 568–574.
16. Bonner, F. T. & Stedman, G. (1996) *Methods in Nitric Oxide Research* (Wiley, New York), pp. 1–18.
17. Pires, M., Ross, D. S. & Rossi, M. J. (1994) *Int. J. Chem. Kinet.* **26,** 1207–1227.
18. Challis, B. C. & Kyrtopoulos, S. A. (1978) *J. Chem. Soc. Perkin Trans. 1*, 1296–1302.
19. Goldstein, S. & Czapski, G. (1995) *J. Am. Chem. Soc.* **117,** 12078–12084.
20. Goldstein, S. & Czapski, G. (1996) *J. Am. Chem. Soc.* **118,** 3419–3425.
21. Kissner R., Nauser, T., Bugnon, P., Lye, P. G. & Koppenol, W. H. (1997) *Chem. Res. Toxicol.* **10,** 1285–1292.
22. Huie, R. E. & Padmaja, S. (1993) *Free Radical Res. Commun.* **18,** 195–199.
23. Koppenol, W. H., Moreno, J. J., Pryor, W. A., Ischiropoulos, H. & Beckman, J. S. (1992) *Chem. Res. Toxicol.* **5,** 834–842.
24. Goldstein, S. & Czapski, G. (1995) *Free Radical Res. Commun.* **19,** 505–510.
25. Beckman, J. S. & Crow, J. P. (1995) *Adv. Pharmacol.* **34,** 17–43.
26. Pryor, W. A. & Squadrito, G. L. (1995) *Am. J. Physiol.* **268,** L699–L722.
27. Ischiropoulos, H. (1998) *Arch. Biochem. Biophys.* **356,** 1–11.
28. Radi, R., Peluffo, G., Alvarez, M. N., Naviliat, M. & Cayota, A. (2001) *Free Radical Biol. Med.* **30,** 463–488.
29. Olson, J. S., Ballou, D. P., Palmer, G. & Massey, V. (1974) *J. Biol. Chem.* **249,** 4350–4362.
30. McCord, J. M. & Fridovich, I. (1969) *J. Biol. Chem.* **244,** 6049–6055.
31. Hrabie, J. A., Klose, J. R., Wink, D. A. & Keefer, L. K. (1993) *J. Org. Chem.* **58,** 1472–1476.
32. Nims, R. W., Darbyshire, J. F., Saavedra, J. E., Christodoulou, D., Hanbauer, I., Cox G. W., Grisham, M. B., Laval, F., Cook, J. A., Krishna, M. C. & Wink, D. A. (1995) *Methods* **7,** 48–54.
33. Christodoulou, D., Kudo, S., Cook, J. A., Krishna, M. C., Miles, A., Grisham, M. B., Murugesan, M., Ford, P. C. & Wink, D. A. (1996) *Methods Enzymol.* **268,** 69–83.
34. Espey, M. G., Miranda, K. M., Pluta, R. M. & Wink, D. A. (2000) *J. Biol. Chem.* **275,** 11341–11347.
35. Espey, M. G., Miranda, K. M., Thomas, D. D. & Wink, D. A. (2001) *J. Biol. Chem.* **276,** 30085–30091.
36. Miles, A. M., Wink, D. A., Cook, J. C. & Grisham, M. B. (1996) *Methods Enzymol.* **268,** 105–120.
37. Kojima, H., Nakatsubo, N., Kikuchi, K., Kawahara, S., Kirino, Y., Nagoshi, H., Hirata, Y. & Nagano, T. (1998) *Anal. Chem.* **70,** 2446–2453.
38. Espey, M. G., Miranda, K. M., Thomas, D. D. & Wink, D. A. (2002) *Free Radical Biol. Med.*, in press.
39. Lymar, S. V., Jiang, Q. & Hurst, J. K. (1996) *Biochemistry* **35,** 7855–7861.
40. Khairutdinov, R. F., Coddington, J. W. & Hurst, J. K. (2000) *Biochemistry* **39,** 14238–14249.
41. Denicola, A., Freeman, B. A., Trujillo, M. & Radi, R. (1996) *Arch. Biochem. Biophys.* **333,** 49–58.
42. Romero, N., Denicola, A., Souza, J. M. & Radi, R. (1999) *Arch. Biochem. Biophys.* **368,** 23–30.
43. Zhang, H., Joseph, J., Feix, J., Hogg, N. & Kalyanaraman, B. (2001) *Biochemistry* **40,** 7675–7686.
44. Jourd'heuil, D., Miranda, K. M., Kim, S. M., Espey, M. G., Vodovotz, Y., Laroux, S., Mai, C. T., Miles, A. M., Grisham, M. B. & Wink D. A. (1999) *Arch. Biochem. Biophys.* **365,** 92–100.
45. Fridovich, I. (1997) *J. Biol. Chem.* **272,** 18515–18517.
46. Granger, D. N. (1988) *Am. J. Physiol.* **255,** H1269–H1275.
47. Yokoyama, Y., Beckman, J. S., Beckman, T. K., Wheat, J. K., Cash, T. G., Freeman, B. A. & Parks, D. A. (1990) *Am. J. Physiol.* **258,** G564–G570.
48. Radi, R., Rubbo, H., Bush, K. & Freeman, B. A. (1997) *Arch. Biochem. Biophys.* **339,** 125–135.
49. Houston, M., Estevez, A., Chumley, P., Aslan, M., Marklund, S., Parks, D. A. & Freeman, B. (1999) *J. Biol. Chem.* **274,** 4985–4994.
50. Espey, M. G., Xavier, S., Thomas, D. D., Miranda, K. M. & Wink, D. A. (2002) *Proc. Natl. Acad. Sci. USA* **99,** 3481–3486.
51. Miles, A. M., Bohle, D. S., Glassbrenner, P. A., Hansert, B., Wink D. A. & Grisham, M. B. (1996) *J. Biol. Chem.* **271,** 40–47.
52. Daiber, A., Frein, D., Namgaladze, D. & Ullrich, V. (2002) *J. Biol. Chem.* 11882–11888.
53. Rubbo, H., Radi, R., Trujillo, M., Telleri, R., Kalyanaraman, B., Barnes, S., Kirk, M. & Freeman, B. A. (1994) *J. Biol. Chem.* **269,** 26066–26075.
54. Pfeiffer, S. & Mayer, B. (1998) *J. Biol. Chem.* **273,** 27280–27285.
55. Wink, D. A., Cook, J. A., Kim, S., Vodovotz, Y., Pacelli, R., Krishna, M. C., Russo, A., Mitchell, J. B., Jourd'heuil, D., Miles, A. M. & Grisham, M. B. (1997) *J. Biol. Chem.* **272,** 11147–11151.
56. Radi, R., Beckman, J. S., Bush, K. M. & Freeman, B. A. (1991) *J. Biol. Chem.* **266,** 4244–4250.
57. Moro, M. A., Darley-Usmar, V. M., Goodwin, D. A., Read, N. G., Zamora-Pino, R., Feelisch, M., Radomski, M. W. & Moncada, S. (1994) *Proc. Natl. Acad. Sci. USA* **91,** 6702–6706.
58. Challis, B. C. & Outram, J. R. (1978) *J. Chem. Soc. Chem. Commun.*, 707–708.
59. Williams, D. L. H. (1997) *Nitric Oxide* **1,** 522–527.
60. Goldstein, S., Czapski, G., Lind, J. & Merenyi, G. (1998) *Inorg. Chem.* **37,** 3943–3947.
61. Gerasimov, O. V. & Lymar, S. V. (1999) *Inorg. Chem.* **37,** 4317–4321.
62. Koppenol, W. H. & Kissner, R. (1998) *Chem. Res. Toxicol.* **11,** 87–90.
63. Stanbury, D. M. (1989) *Adv. Inorg. Chem.* **33,** 69–139.
64. Denicola, A., Souza, J. M. & Radi, R. (1998) *Proc. Natl. Acad. Sci. USA* **95,** 3566–3571.
65. Caulfield, J. L., Singh, S. P., Wishnok, J. S., Deen, W. M. & Tannenbaum, S. R. (1996) *J. Biol. Chem.* **271,** 25859–25863.
66. Liu, X., Miller, M. J., Joshi, M. S., Thomas, D. D. & Lancaster, J. R., Jr. (1998) *Proc. Natl. Acad. Sci. USA* **95,** 2175–2179.
67. Miles, A. M., Gibson, M. F., Kirshina, M., Cook, J. C., Pacelli, R., Wink, D. A. & Grisham, M. B. (1995) *Free Radical Res.* **23,** 379–390.
68. Wung, B. S., Cheng, J. J., Shyue, S. K. & Wang, D. L. (2001) *Arterioscler. Thromb. Vasc. Biol.* **21,** 1941–1947.
69. Chiu, J. J., Wung, B. S., Hsieh, H. J., Lo, L. W. & Wang, D. L. (1999) *Circ. Res.* **85,** 238–246.
70. Ghafourifar, P., Schenk, U., Klein, S. D. & Richter, C. (1999) *J. Biol. Chem.* **274,** 31185–31188.
71. Wink, D. A., Hanbauer, I., Krishna, M. C., DeGraff, W., Gamson, J. & Mitchell, J. B. (1993) *Proc. Natl. Acad. Sci. USA* **90,** 9813–9817.
72. Wink, D. A., Miranda, K. M., Espey, M. G., Pluta, R. M., Colton, C., Vitek, M., Feelisch, M. & Grisham, M. B. (2001) *Antiox. Redox Signal.* **3,** 203–213.